DEMOSAICKING IMAGES WITH MOTION BLUR

Shay Har-Noy, Stanley H. Chan, and Truong Q. Nguyen

UC - San Diego, ECE Dept.
http://videoprocessing.ucsd.edu
harnoy@alumni.rice.edu, h5chan@ucsd.edu, nguyent@ece.ucsd.edu

ABSTRACT

In standard digital color imaging, each pixel position acquires data for only one color plane and the remaining two color planes must be inferred through a process known as demosaicking. Furthermore, the image is susceptible to blurring artifacts due to a moving camera or fast moving subject. In this work we develop a robust framework to demosaick the color filter array (CFA) image while reducing the blur corrupting the image. We begin by defining a color motion blur model that describes the motion blur artifacts affecting color images. We then integrate the motion blur model in the demosaicking algorithm to obtain a computationally efficient framework for deblurring while demosaicking.

Index Terms— Cameras, image restoration, image sensors.

1. INTRODUCTION

The typical digital image acquisition pipeline uses a single sensor along with a color filter array (CFA) that captures only one component at each spatial location (e.g. the Bayer Pattern [1]). Demosaicking algorithms that leverage the spatial and spectral redundancies in the image are then applied to the $M \times N$ output of the CFA to produce an $M \times N \times 3$ color image (see [2] for a review).

Traditional image demosaicking methods usually do not consider the blurring artifacts and assume that the "known" $M \times N$ pixels are accurate. Furthermore, image restoration [3] techniques typically assumes that no demosaicking took place and that all $M \times N \times 3$ pixels are accurate. In this paper we consider the problem of joint deblurring and demosaicking where both of these assumptions are broken. The fundamental tradeoff between temporal and spatial resolution [4] causes the problem of motion blur to be particularly relevant. As the density of pixels on a CCD sensor increases, the size of each pixel gets smaller and therefore so does the amount of light hitting the sensor at each pixel location. In order to maintain a high SNR at each pixel location, the exposure time must therefore be increased leading to motion blur in the case of camera or subject motion. Indeed, demosaicking and deblurring has been previously discussed in a few prior works [5–8], to which we will compare our results.

The proposed deblurring-demosaicking framework uses recently developed methods of CFA signal decomposition [9, 10] to extract the $M \times N$ luminance image. The estimate of the luminance image is then sharpened using any image deblurring technique with the result combined with an estimate of the demosaicked color image to form a final color image consistent with the deblurred $M \times N$ luminance image. Due to the flexibility in choosing the demosaicking and deblurring methods, the algorithm is able to utilize both the state of the art demosaicking techniques and image restoration techniques based on the computational constraints of the application and desired perceptual performance.

In section 2 we introduce a model for motion blur in color images acquired with a digital camera using a CFA. Section 3 discusses demosaicking in the frequency domain along with a method to extract the full resolution luminance component. Section 4 introduces an algorithm that combats blurring artifacts during the demosaicking process. We apply our method to natural and simulated images to show its effectiveness in section 5.

2. COLOR MOTION BLUR MODEL

Having an accurate motion blur model allows us to quantify improvements provided by algorithms aimed at reducing motion blur. As the exposure time on a digital imaging device becomes longer, a scene with significant motion will be more likely to blur across multiple sensor pixels. Consider a filter bank operating on a row of the "true" color channel of an image, $C(z)$, that suffers from motion blur (Fig. 1). The color channel is first downsampled by 2 at which point a blurring kernel, $H_c(z)$, is applied. The blurred and downsampled color channel is then upsampled and interpolated/demosaicked using some some filter $F(z)$. Although most modern demosaicking algorithms rely on the inter-channel redundancies in a CFA image to improve demosaicking, for our purposes the simple model will suffice.

This work is supported by Broadcom Corporation and UC Discovery. The authors would like to thank Quang Dam Le, Sunkwang Hong for their assistance and support. Also Dr. Keigo Hirakawa for his insight and for providing assistance in gathering relevant code and sample images.

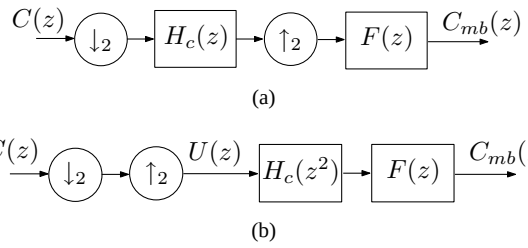

Fig. 1. Two equivalent filter banks depicting horizontal motion blur on a row captured using a Bayer color filter.

This filter model allows us to write an expression for the final blurred color channel:

$$C_{mb}(z) = \frac{1}{2}\left[C(z) + C(-z)\right] H_c(z^2) F(z) \qquad (1)$$

where $H_c(z)$ is the blurring kernel that depends on the motion in the scene and may depend on the color channel. Consequently, to model motion blur in a given image we apply the blurring kernels to each of the channels in the downsampled CFA domain or equivalently apply $H_c(z^2)$ to each of the color channels after demosaicking.

3. CFA SIGNAL DECOMPOSITION

The $M \times N$ multiplexed Bayer CFA image can be interpreted in the frequency domain as a luminance component at baseband and two chrominance components modulated to a higher frequency [9]. Let $f_{CFA}[n_1, n_2]$ be the $M \times N$ Bayer CFA output, $f_L[n_1, n_2]$ the luminance component, and $f_{C1}[n_1, n_2]$ and $f_{C2}[n_1, n_2]$ the two chroma components we get:

$$\begin{aligned} f_{CFA}[n_1, n_2] = f_L[n_1, n_2] + f_{C1}[n_1, n_2](-1)^{n_1+n_2} \\ + f_{C2}[n_1, n_2]\left((-1)^{n_1} - (-1)^{n_2}\right) \end{aligned} \qquad (2)$$

where

$$\begin{pmatrix} f_L \\ f_{C1} \\ f_{C2} \end{pmatrix} = \begin{pmatrix} \frac{1}{4} & \frac{1}{2} & \frac{1}{4} \\ -\frac{1}{4} & \frac{1}{2} & -\frac{1}{4} \\ -\frac{1}{4} & 0 & \frac{1}{4} \end{pmatrix} \begin{pmatrix} f_R \\ f_G \\ f_B \end{pmatrix} \qquad (3)$$

and f_R, f_G, and f_B are the full resolution RGB color planes. Fig. 2 shows the approximate locations of the modulated chroma and baseband luminance components in the frequency domain. The demosaicking algorithm presented in [10] operates by extracting the luminance component, f_L, and demodulating the chroma components (i.e. extract f_{C1} and f_{C2}) allowing it to recover the full resolution $M \times N \times 3$ RGB image using the inverse of the matrix in eq. (3). The optimal filter coefficients for extracting these signals can be obtained by minimizing the total squared error between the true components f_L, f_{C1}, f_{C2} and the estimated ones $\hat{f}_L$, $\hat{f}_{C1}$, $\hat{f}_{C2}$ over a training set. In our algorithm, we use the optimal coefficients computed in [10] to extract a high quality estimate of the luminance image.

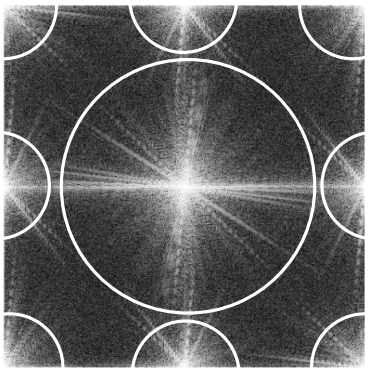

Fig. 2. FFT of a Bayer CFA image with approximate locations of the luminance and chrominance components.

4. DEBLURRING DURING DEMOSAICKING

The proposed deblurring and demosaicking framework sharpens the luminance image extracted using the method described in section 3 and combines it with an estimate of the standard demosaicked image. The combination is performed by choosing the final sharp color planes, $\hat{f}_R^{sh}$, $\hat{f}_G^{sh}$, $\hat{f}_B^{sh}$, such that they are close to the demosaicked result, i.e. $\hat{f}_R^{sh} \approx \hat{f}_R$, $\hat{f}_G^{sh} \approx \hat{f}_G$, $\hat{f}_B^{sh} \approx \hat{f}_B$, while still being consistent with the estimate for the sharpened luminance component. More precisely:

$$\begin{aligned} &\underset{\hat{f}_R^{sh}, \hat{f}_G^{sh}, \hat{f}_B^{sh}}{\text{argmin}} \; \|\hat{f}_R^{sh} - \hat{f}_R\|_2^2 + \|\hat{f}_G^{sh} - \hat{f}_G\|_2^2 + \|\hat{f}_B^{sh} - \hat{f}_B\|_2^2 \\ &\text{subject to} \quad \frac{\hat{f}_R^{sh} + 2\hat{f}_G^{sh} + \hat{f}_B^{sh}}{4} = \hat{f}_L^{sh}. \end{aligned} \qquad (4)$$

Notice that there are no spatial dependencies between the pixels in eq. (4) and thus we can solve the procedure element by element through a non-iterative solution using Lagrange multipliers:

$$\begin{aligned} \Lambda(\hat{f}_R^{sh}, \hat{f}_G^{sh}, \hat{f}_B^{sh}, \lambda) &= (\hat{f}_R^{sh} - \hat{f}_R)^2 + (\hat{f}_G^{sh} - \hat{f}_G)^2 \\ &+ (\hat{f}_B^{sh} - \hat{f}_B)^2 + \lambda\left(\hat{f}_L^{sh}[i,j] - \frac{\hat{f}_R^{sh} + 2\hat{f}_G^{sh} + \hat{f}_B^{sh}}{4}\right). \end{aligned}$$

To find the minimum of the above equation we set its scalar partial derivatives equal to 0 and solve the system of equations to arrive at the optimal result:

$$\begin{pmatrix} \hat{f}_R^{sh} \\ \hat{f}_G^{sh} \\ \hat{f}_B^{sh} \\ \lambda \end{pmatrix} = \begin{pmatrix} \frac{5}{6} & -\frac{1}{3} & -\frac{1}{6} & \frac{2}{3} \\ -\frac{1}{3} & \frac{1}{3} & -\frac{1}{3} & \frac{4}{3} \\ -\frac{1}{6} & -\frac{1}{3} & \frac{5}{6} & \frac{2}{3} \\ -\frac{4}{3} & -\frac{8}{3} & -\frac{4}{3} & \frac{16}{3} \end{pmatrix} \begin{pmatrix} \hat{f}_R \\ \hat{f}_G \\ \hat{f}_B \\ \hat{f}_L^{sh} \end{pmatrix}. \qquad (5)$$

Thus the optimal final image can be obtained through a linear combination of the estimates of the RGB image $\{\hat{f}_R$,

$\hat{f}_G$, $\hat{f}_B\}$, and the deblurred luminance image $\hat{f}_L^{sh}$ using eq. (5) (Fig. 3).

Algorithm 1 Demosaick Deblurring Algorithm

Given a blurry $M \times N$ Bayer CFA image, and the blurring PSF:

1. Obtain an estimate of luminance component $\hat{f}_L$ using the approach detailed in section 3.
2. Sharpen the estimate of the luminance component to form $\hat{f}_L^{sh}$ using any image deblurring algorithm.
3. Form an estimate of the demosaicked $M \times N \times 3$ RGB image $\{\hat{f}_R, \hat{f}_G, \hat{f}_B\}$ using any fast demosaicking algorithm.
4. Combine the sharp luminance component $\hat{f}_L^{sh}$, and the blurred demosaicked RGB color planes according to eq. (5).

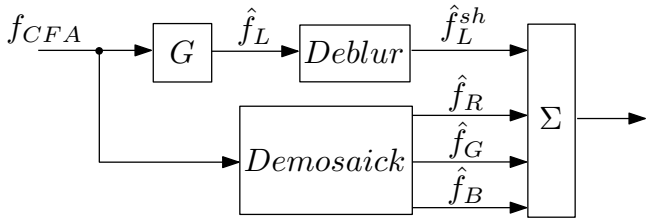

Fig. 3. Block diagram of the proposed algorithm. The block labelled G corresponds to the procedure detailed in section 3 to extract an estimate of the luminance component.

Fig. 3 shows a block diagram of Alg. 1 where we are able to choose both the demosaicking and deblurring algorithms based on our complexity constraints and desired perceptual quality.

5. SIMULATION RESULTS

5.1. Natural Motion Blur

To assess the effectiveness of Alg. 1 in a real world application we acquired images using a commercial digital camera where we introduced significant panning camera motion and chose an appropriate exposure time to create the motion blur artifact. Alg. 1 was then applied to the acquired blurry mosaicked image. For deblurring-demosaicking purposes, the length of the motion blur filter was chosen based on amount of perceived blur in the image and the direction was known a priori.

The demosaicking procedure used in Fig. 4 was the procedure described in [10] with the optimal filter coefficients derived based on all of the images in the Kodak dataset[1]. These optimal coefficients were also used for extracting the $\hat{f}_L$ estimate to which a total variation deblurring procedure was applied [11].

5.2. Simulated Results

To quantify the perceptual improvements seen in Fig. 4 we simulate motion blur on the standard Kodak set of images [12] using a known blurring kernel to the images as described in section 2 to simulate a Bayer I_{CFA} acquired with a moving camera. The blurring kernel had a length of 5 and had a non-zero response time. We found that applying the perfect box blurring kernel had little effect on the objective or subjective results.

To obtain an objective measure of quality we calculate the PSNR of each of the demosaicked RGB color planes as well as the SCIELAB ΔE_{ab}^* distance [13], Structural SIMilarity Index [14] (SSIM) metric averaged across all three RGB color planes ($\bar{Q}$), and the color extension to SSIM (Q_{color}) [15]. A lower ΔE_{ab}^* indicates better quality whereas a higher value for all of the other metrics indicates better quality.

Table 1 shows the performance of Alg. 1 implemented with the TV deblurring method and the demosaicking procedure described in [10][2] compared to demosaicking alone and the joint demosaicking-deblurring method of [8]. The optimal filter coefficients used to extract the $\{\hat{f}_L, \hat{f}_{C1}, \hat{f}_{C2}\}$ images from I_{CFA} were rederived using the first twelve images in the Kodak dataset. The results indicate that Alg. 1 offers improvements over simple demosaicking and the joint deblurring-demosaicking method described in [8].

6. CONCLUSION

In this work we developed a framework for joint demosaicking and deblurring of images acquired using a color filter array (CFA). The framework leverages models of color motion blur and recent advances in CFA signal decomposition and is able to leverage state-of-the-art image restoration and demosaicking techniques. Objective and subjective results both indicate that the presented algorithm indeed reduce the amount of blur visible in the image and improves the image quality.

7. REFERENCES

[1] B.E. Bayer, *Color imaging Array*, U.S. Patent 3971065, 1976.

[2] B.K. Gunturk, J. Glotzbach, Y. Altunbasak, R.W. Schafer, and R.M. Mersereau, "Demosaicking: color

[1] The authors would like to express their gratitude to E. Dubois for making his code available and offering suggestions.

[2] Additional full resolution results and a sample implementation are available at: http://videoprocessing.ucsd.edu/∼sharnoy/IEEETranDemosaick/

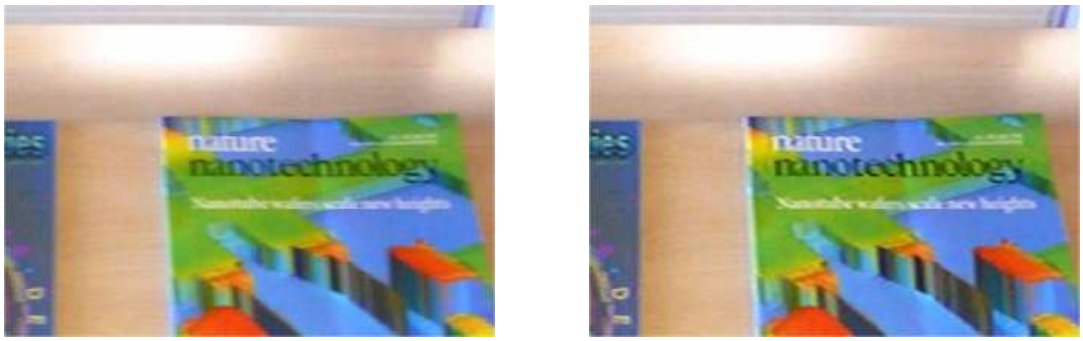

Fig. 4. Natural image acquired with a moving digital camera comparing the output of Alg. 1 (right) and the demosaicking procedure described in [10] (left).

Table 1. A sample of the objective results showing the performance of Alg. 1 on the Kodak data set.

Image	Method	ΔE^*_{ab}	$\bar{Q}$	Q_{color}	$PSNR_R$	$PSNR_G$	$PSNR_B$
Airplane	Alg. 1	2.02	0.85	0.83	27.7 dB	28.2 dB	27.9 dB
	[8]	2.74	0.81	0.77	25.8 dB	26.8 dB	25.4 dB
	[10]	2.29	0.83	0.79	26.9 dB	26.9 dB	27.3 dB
Lighthouse	Alg. 1	2.63	0.83	1.21	26.5 dB	27.0 dB	26.9 dB
	[8]	3.69	0.75	1.03	24.3 dB	26.0 dB	24.2 dB
	[10]	3.01	0.80	1.15	25.8 dB	25.8 dB	26.2 dB
House	Alg. 1	4.01	0.70	1.14	24.4 dB	24.1 dB	23.3 dB
	[8]	4.85	0.63	0.99	23.2 dB	23.6 dB	21.5 dB
	[10]	4.60	0.64	1.03	23.7 dB	23.0 dB	22.7 dB

filter array interpolation," *Signal Processing Magazine, IEEE*, 2005.

[3] Peter A. Jansson, Ed., *Deconvolution of Images and Spectra*, Academic Press, 2nd edition, 1997.

[4] S.K. Nayar and M. Ben-Ezra, "Motion-based motion deblurring," *Pattern Analysis and Machine Intelligence, IEEE Transactions on*, 2004.

[5] Mejdi Trimeche, Dmitry Paliy, Markku Vehvilainen, and Vladimir Katkovnic, "Multichannel image deblurring of raw color components," in *Proc. SPIE*, San Jose, CA, USA, Mar. 2005, vol. 5674, pp. 169–178, SPIE.

[6] Dmytro Paliy, Alessandro Foi, Radu Bilcu, Vladimir Katkovnik, and Karen Egiazarian, "Joint deblurring and demosaicing of poissonian bayer-data based on local adaptivity," in *Signal Processing, 2008. EUSIPCO. European Conference on*, 2008.

[7] J. Portilla, D. Otaduy, and C. Dorronsoro, "Low-complexity linear demosaicing using joint spatial-chromatic image statistics," in *Image Processing, 2005. ICIP 2005. IEEE International Conference on*, 2005.

[8] Takashi Komatsu and Takahiro Saito, "Demosaicking for a color image sensor with removal of blur due to an optical low-pass filter," in *Proceedings of SPIE*, 2004.

[9] D. Alleysson, S. Susstrunk, and J. Herault, "Linear demosaicing inspired by the human visual system," *Image Processing, IEEE Transactions on*, 2005.

[10] E. Dubois, "Filter design for adaptive frequency-domain bayer demosaicking," in *Image Processing, 2006 IEEE International Conference on*, 2006.

[11] Stanley H. Chan and Truong Q. Nguyen, "Lcd motion blur: Model, analysis and algorithm," *Image Processing, IEEE Transactions on*, (Submitted).

[12] 40 Scanned Images, "Eastman Kodak photographic color image database," 1993.

[13] Xuemei Zhang, Brian A. Wandell, and Brian A. W, "A spatial extension of CIELAB for digital color image reproduction," in *Proc. of the SID Symposiums*, 1996.

[14] Zhou Wang, A.C. Bovik, H.R. Sheikh, and E.P. Simoncelli, "Image quality assessment: from error visibility to structural similarity," *Image Processing, IEEE Transactions on*, 2004.

[15] Alexander Toet and Marcel P. Lucassen, "A new universal colour image fidelity metric," *Elsevier Displays*, Dec. 2003.